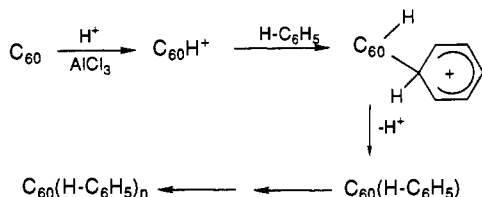


Similar results were also obtained with pure  $C_{60}$ .<sup>16b</sup> Similar reaction with toluene gave toluene addition products. The FAB mass spectrum showed  $M^+$  at 1824, indicating the formation of  $C_{60}(C_6H_5-CH_3)_{12}$ . In this case, too, consecutive loss of toluene ( $m/e$  92) was observed all the way to  $C_{60}(C_6H_5-CH_3)_2$ . In the 300-MHz  $^1H$  NMR spectrum (Figure 1) ( $CDCl_3$ ), absorptions at  $\delta(^1H)$  7.2 (broad),  $\delta(^1H)$  4.5 (extremely broad), and  $\delta(^1H)$  2.35 (broad) are observed. The spectrum is in accord with poly-toluenefullerenes. Relative integration of the proton signals at  $\delta(^1H)$  7.2 and 4.5 gave a ratio of 4:1, indicating only monosubstitution of toluene (in all probability in the para position).

The reaction takes place only under relatively strong Friedel-Crafts acid catalysis. Weak Lewis acids such as stannic chloride or titanium tetrachloride did not catalyze the reaction. The reaction can be rationalized by initial protonation (by the residual protons in  $AlCl_3$ ) of fullerene to fullerene cation followed by electrophilic fullereneation of the aromatic. The sequence repeats till on the average 12 Ar-H units are added. The reaction is similar to alkylation by alkenes (polyenes) under acidic catalysis. We are in the process of investigating this interesting mechanism more thoroughly. Redox processes, particularly with more easily reducible Lewis acid halide ( $FeCl_3$ ,  $SbF_5$ , etc.) catalyzed reactions, can also be operative, involving single electron transfer (SET).



A fullerene  $C_{60}/C_{70}$  mixture was also found to undergo reaction with non-cross-linked polystyrene<sup>18</sup> under aluminum trichloride catalysis in  $CS_2$  solvent to fullereneated polystyrene of a highly cross-linked nature. We are continuing our investigations on polyarenefullerenes and their intriguing reactions.

**Acknowledgment.** Support of the work at USC by the National Institutes of Health and the National Science Foundation is gratefully acknowledged.

(18) We thank Professor T. Hogen-Esch for a sample of monodispersed non-cross-linked polystyrene (mol wt  $\approx$  8500).

## Mechanism of Adenylate Kinase. 12. Prediction and Demonstration of Enhancement of Phosphorus Stereospecificity by Site-Directed Mutagenesis<sup>1</sup>

Terri Dahnke, Ru-Tai Jiang, and Ming-Daw Tsai\*

Department of Chemistry, The Ohio State University  
Columbus, Ohio 43210

Received August 12, 1991

Recently we have demonstrated a reversal of stereospecificity<sup>2</sup> for the R44M (Arg-44 to Met) mutant enzyme of adenylate kinase (AK, from chicken muscle, overproduced in *Escherichia coli*).<sup>3,4</sup> We now report an enhancement of stereospecificity in the conversion of AMPS to ADP $\alpha$ S catalyzed by R97M (Arg-97 to Met) mutant AK, entirely based upon rational prediction.

(1) Supported by Research Grant DMB-8904727 from the NSF. Paper 11; Reference 4. Abbreviations: ADP, adenosine 5'-diphosphate; ADP $\alpha$ S, adenosine 5'-O-(1-thiodiphosphate); AK, adenylate kinase; AMP, adenosine 5'-monophosphate; AMPS, adenosine 5'-monothiophosphate; AP $_3$ A, P $_1$ , P $_2$ , b $_3$ (5'-adenosyl)pentaphosphate; ATP, adenosine 5'-triphosphate; ATP $\alpha$ S, adenosine 5'-O-(1-thiotriphosphate); WT, wild type.

(2) Jiang, R.-T.; Dahnke, T.; Tsai, M.-D. *J. Am. Chem. Soc.* 1991, 113, 5485-5486.

(3) Tanizawa, Y.; Kishi, F.; Kaneko, T.; Nakazawa, A. *J. Biochem. (Tokyo)* 1987, 101, 1289-1296.

(4) Tsai, M.-D.; Yan, H. *Biochemistry* 1991, 30, 6806-6818.

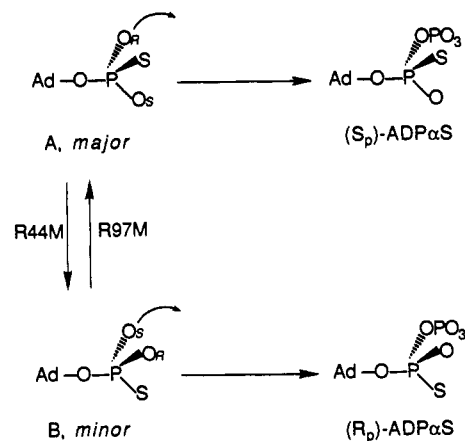


Figure 1. Schemes showing the major and minor conformers of AMPS at the active site of WT and the conversion of these conformers to ADP $\alpha$ S. The equilibrium is shifted to conformer B upon R44M mutation and to conformer A upon R97M mutation. It should be noted that a third, nonproductive conformer (with sulfur positioned at the acceptor position) could also be present in WT and both mutants.

The WT AK is known to convert AMPS to  $(S_p)$ -ADP $\alpha$ S specifically at the AMP site,<sup>2,5</sup> which is in turn converted to  $(S_p)$ -ATP $\alpha$ S specifically at the MgATP site.<sup>2,6</sup> However, the stereospecificity is not 100% in either case. Under various conditions, we have detected 5-10% of  $(R_p)$ -ADP $\alpha$ S and <5% of  $(R_p)$ -ATP $\alpha$ S in the reaction mixture. As shown in Figure 1, the stereospecificity at the AMP site can be explained by a major conformer A and a minor conformer B at the active site. For R44M,<sup>2</sup> we predicted a possible change in stereospecificity at the AMP site on the basis of the kinetic data (22-fold increase in the  $K_d$  and 36-fold increase in the  $K_m$  of AMP)<sup>7</sup> and the crystal structures (the yeast AK-MgAP $_3$ A complex<sup>8</sup> and the AK3-AMP complex<sup>9</sup>). However, we were unable to predict how it would change (i.e., relaxation, reversal, or enhancement). The observed dramatic reversal of stereospecificity suggested that Arg-44 plays an important role in orienting the conformation of the phosphorothioate group of bound AMPS. The A to B equilibrium is shifted to B in R44M, as shown in Figure 1.

The crystal structures, however, indicate that another arginine (corresponding to Arg-97 in our system) can also interact with the phosphoryl group of AMP,<sup>8,9</sup> which prompted us to construct the R97M mutant AK. Binding and kinetic analysis yielded 20- and 30-fold increases in the  $K_d$  and  $K_m$  of AMP, respectively, with no significant perturbation in MgATP binding and a 30-fold decrease in  $k_{cat}$ . Structural characterization of this mutant by NMR indicated no significant conformational perturbations. These results established that Arg-97 interacts with AMP during the catalysis by AK and led us to predict a change in the stereospecificity of R97M. Since the side chains of Arg-97 and Arg-44 point toward the phosphoryl group of AMP from opposite sides, we also predicted that R97M and R44M should perturb the stereospecificity in opposite directions, i.e., the stereospecificity of R97M should be enhanced relative to WT.

To prove that a highly stereospecific reaction has been enhanced, one must demonstrate formation of the minor isomer ( $R_p$ ) at the early stage of reaction for WT, and lack of (or decreased) formation of the  $R_p$  isomer at a later stage of reaction for R97M.

(5) Sheu, K.-F. R.; Frey, P. A. *J. Biol. Chem.* 1977, 252, 4445-4448.

(6) (a) Eckstein, F.; Goody, R. S. *Biochemistry* 1976, 15, 1685-1691. (b) Eckstein, F.; Romaniuk, P. J.; Connolly, B. A. *Methods Enzymol.* 1982, 87, 197-212. (c) Tomasselli, A. G.; Noda, L. H. *Fed. Proc.* 1981, 40, 1864. (d) Kalbitzer, H. R.; Marquetant, R.; Connolly, B. A.; Goody, R. S. *Eur. J. Biochem.* 1983, 133, 221-227. (e) Tomasselli, A. G.; Noda, L. H. *Eur. J. Biochem.* 1983, 132, 109-115.

(7) Yan, H.; Dahnke, T.; Zhou, B.; Nakazawa, A.; Tsai, M.-D. *Biochemistry* 1990, 29, 10956-10964.

(8) Egner, U.; Tomasselli, A. G.; Schulz, G. E. *J. Mol. Biol.* 1987, 195, 649-658.

(9) Diederichs, K.; Schulz, G. E. *Biochemistry* 1990, 29, 8138-8144.

(10) Jaffe, E. K.; Cohn, M. *Biochemistry* 1978, 17, 652-657.

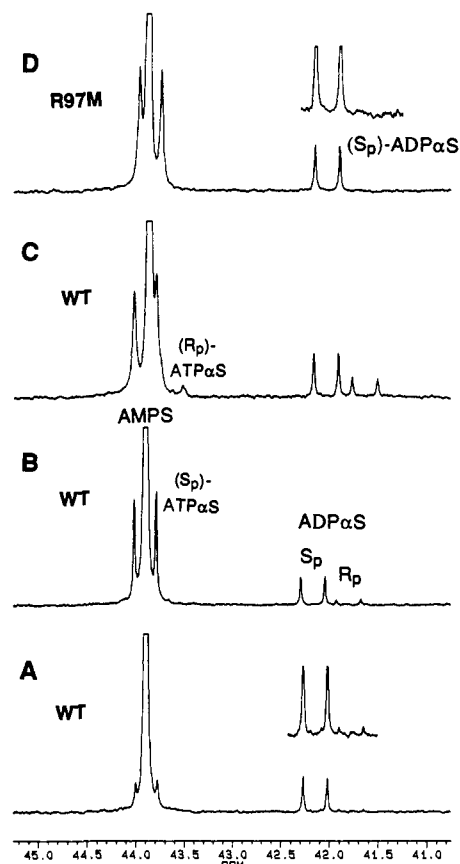


**Figure 2.**  $^{31}\text{P}$  NMR spectra showing the conversion of AMPS to ADP $\alpha$ S (and subsequent conversion to ATP $\alpha$ S). Only the  $\text{P}_\alpha$  resonances are shown. (A–C) WT AK, after 9%, 17%, and 29%, respectively, of AMPS has reacted. (D) R97M, at 27% conversion. Spectra were obtained after addition of 100 mM EDTA and 150  $\mu\text{L}$  of triethylamine to optimize for the detection of ADP $\alpha$ S. Except for sample C, no ( $R_p$ )-ATP $\alpha$ S was detectable even under other conditions, optimized for the detection of ADP $\alpha$ S (spectra not shown). The intensities of various components described in the text were measured by cutting and weighing from greatly expanded spectra. The assignments of different species have been confirmed by mixing with known compounds and agree with previous reports.<sup>5,10</sup> The starting reaction mixture (600  $\mu\text{L}$ ) consisted of 22 mM AMPS, 75 mM ATP, and 80 mM  $\text{MgCl}_2$ , in a 50 mM Tris buffer containing 50 mM KCl, 2.5 mM EDTA, and 15%  $\text{D}_2\text{O}$ , pH = 7.8. The broadband decoupled spectra were obtained at 121.5 MHz with a pulse width of 45°. The acquisition time was 1.5 s, the repetition time was 2 s, and ca. 23 000 transients were accumulated for each spectrum. The FID was processed with 2.0-Hz exponential multiplication.

These were accomplished by  $^{31}\text{P}$  NMR analysis as shown in Figure 2. Spectra A, B, and C are the reaction mixtures of WT after 9%, 17%, and 29%, respectively, of AMPS has been converted to products. The minor isomer, ( $R_p$ )-ADP $\alpha$ S, is clearly detectable in these spectra and constitutes 5%, 15%, and 28%, respectively, of the total ADP $\alpha$ S, or 0.27%, 0.54%, and 1.7%, respectively, of the starting AMPS. In D, 27% of AMPS has been converted to products by R97M, but no ( $R_p$ )-ADP $\alpha$ S can be detected. If there was no change in stereospecificity, sample D should have consisted of more than 0.54% but less than 1.7% of the  $R_p$  isomer relative to the starting AMPS (the 1.7% of spectrum C could be an overestimation since the reaction has passed equilibrium). If we take a conservative value of 1%, the  $R_p$  isomer in D should have been 3–4 times that in A. Since the signal/noise ratios in D and A are comparable and the signal/noise ratio of ( $R_p$ )-ADP $\alpha$ S in A is ca. 3, formation of the  $R_p$  isomer has decreased at least 10-fold in D. These results and analysis indicate an enhancement of stereospecificity in R97M relative to WT, i.e., the A to B equilibrium has been shifted to A in R97M, as also indicated in Figure 1.

In terms of molecular events at the active site, the two arginine side chains appear to “compete” for the nonbridging sulfur and/or

oxygen. Such competing interactions should start at the AK-AMPS binary complex and persist through the transition state. The balance between the two competing interactions results in the observed stereospecificity in WT, which is shifted one way or the other upon removal of one of the two interactions. Since the major conformer has been perturbed upon R44M mutation, Arg-44 appears to “win” over Arg-97 in orienting the phosphorothioate. The molecular detail of such interactions, however, remains to be established.

## Ab Initio Study of Spiropentadiene, $\text{C}_5\text{H}_4$

Isaiah Shavitt\* and David W. Ewing†

Department of Chemistry, The Ohio State University  
Columbus, Ohio 43210

Janet E. Del Bene\*

Department of Chemistry, Youngstown State University  
Youngstown, Ohio 44555

Received July 22, 1991

In a recent paper, Billups and Haley<sup>1</sup> reported the synthesis of spiropentadiene, the simplest small-ring, spiro-connected cycloalkene. Because of its high endothermicity, it was not possible for these investigators to characterize spiropentadiene structurally or spectroscopically. A previous ab initio theoretical study of spiropentadiene has been reported,<sup>2</sup> but was carried out at the Hartree-Fock (HF) level of theory with small basis sets. In our recent work we have been investigating basis set, correlation, and geometry effects on the stabilities of hydrocarbons and carbocations.<sup>3</sup> We now extend this work to the prediction of the structure, vibrational frequencies, and standard heat of formation of spiropentadiene.

The structure of spiropentadiene has been optimized with  $D_{2d}$  symmetry constraints at second-order many-body Møller-Plesset perturbation theory<sup>4–9</sup> [MBPT(2)  $\equiv$  MP2] using the 6–31+G(d,p) basis set.<sup>10–13</sup> Harmonic vibrational frequencies were computed to ensure that this structure is a local minimum, to obtain both zero-point and thermal vibrational energies, and to predict the vibrational spectrum. A single-point calculation at fourth-order perturbation theory including triple excitations [MBPT(4)] was carried out at the optimized MP2/6-31+G(d,p) geometry using the much larger Dunning correlation-consistent polarized valence triple- $\zeta$  basis set (cc-pVTZ).<sup>14</sup> The cc-pVTZ basis set contains two sets of first polarization functions and a single set of second polarization functions on each atom. The MP2/6-31+G(d,p) structure optimization and frequencies calculations were done using the Gaussian 90 system of computer programs.<sup>15</sup> The cc-pVTZ

† Present address: Department of Chemistry, John Carroll University, Cleveland, OH 44118.

- (1) Billups, W. E.; Haley, M. M. *J. Am. Chem. Soc.* **1991**, *113*, 5084.
- (2) Kao, J.; Radom, L. *J. Am. Chem. Soc.* **1978**, *100*, 760.
- (3) Del Bene, J. E.; Aue, D. H.; Shavitt, I. Stabilities of Hydrocarbons and Carbocations. 1. A Comparison of Augmented 631G, 6311G, and Correlation Consistent Basis Sets, submitted to *J. Am. Chem. Soc.*
- (4) Bartlett, R. J.; Silver, D. M. *J. Chem. Phys.* **1975**, *62*, 3258; **1976**, *64*, 1260, 4578.
- (5) Binkley, J. S.; Pople, J. A. *Int. J. Quantum Chem.* **1975**, *9*, 229.
- (6) Pople, J. A.; Binkley, J. S.; Seeger, R. *Int. J. Quantum Chem., Quantum Chem. Symp.* **1976**, *10*, 1.
- (7) Krishnan, R.; Pople, J. A. *Int. J. Quantum Chem.* **1978**, *14*, 91.
- (8) Purvis, G. D.; Bartlett, R. J. *J. Chem. Phys.* **1978**, *68*, 2114.
- (9) Bartlett, R. J.; Purvis, G. D. *Int. J. Quantum Chem.* **1978**, *14*, 561.
- (10) Hariharan, P. C.; Pople, J. A. *Theor. Chim. Acta* **1973**, *28*, 213.
- (11) Dill, J. D.; Pople, J. A. *J. Chem. Phys.* **1975**, *62*, 2921.
- (12) Spitznagel, G. W.; Clark, T.; Chandrasekhar, J.; Schleyer, P. v. R. *J. Comput. Chem.* **1982**, *3*, 363.
- (13) Clark, T.; Chandrasekhar, J.; Spitznagel, G. W.; Schleyer, P. v. R. *J. Comput. Chem.* **1983**, *4*, 294.
- (14) Dunning, T. H., Jr. *J. Chem. Phys.* **1989**, *90*, 1007.